ELECTROSPINNING POLY(LACTIC ACID) WITH A BIMODAL INTER-FIBER PORE SIZE DISTRIBUTION

A Thesis

Presented to the Faculty of the Graduate School

of Cornell University

In Partial Fulfillment of the Requirements for the Degree of

Master of Science

by

Mary Rebovich

February 2010

ABSTRACT

This research concerns the fabrication of electrospun Poly(lactic acid) membranes onto a patterned surface to produce a bimodal pore size distribution as well as the control of fabric properties via control of fiber properties. In the case of patterned electrospinning, a grid substrate was utilized to selectively collect electrospun fibers in desired locations while amassing fewer fibers between the grid wires. Membranes produced from grids with 3mm or 5mm spacing between copper wires possessed bimodal inter-fiber pore size distributions. Membranes produced from grids with 1mm spacing between copper wires had no significant difference in pore size distribution when compared with control samples prepared on flat copper sheets. The pore size distribution affects membrane wettability. It is shown that membranes possessing small pore sizes and small pore size distributions absorb more wetting liquid than membranes with large pore sizes and large pore size distributions. This phenomenon results from capillary action. The capillary action equation can be modified to model the pores as a series of interconnected spheres. Determining the number of pores of a given size remains a challenge, but with an appropriate pore number approximation, this equation has the potential to provide an accurate prediction of absorbency for a given membrane. Fiber morphology and ionicity was altered by modifying applied electrospinning voltage, spinning dope solvent concentration, and ionic filler concentration. These variations did not affect fiber properties significantly enough to alter load sharing in the full membrane; thus, compliance was not significantly affected by changes in fiber qualities.

BIOGRAPHICAL SKETCH

Mary E. Rebovich is a native of Charlotte, NC, and holds a B.S. degree in Materials Science and Engineering from North Carolina State University.

ACKNOWLEDGMENTS

Special thanks to Margaret Frey, Chunhui Xiang, Min Xiao, Lili Li, and Erin Hendrick for all of their support. From the MS&E department, I would to thank Lara Estroff. I would also like to recognize John Hunt for his assistance.

TABLE OF CONTENTS

LIST OF FIGURES

LIST OF TABLES

INTRODUCTION

Originally developed in the 1930's, electrospinning is a fiber formation process in which a charged polymer solution droplet elongates into a fiber and deposits onto a grounded or oppositely charged substrate by static repulsion (Gladding). Electrospun membrane fabrication requires control of spinning conditions including solvent quality, solvent concentration, solution flow rate, voltage supplied, needle to collector distance, and viscosity (Salem). For ease of explanation, these parameters can be grouped into solution parameters and process parameters.

Solvent quality specifically refers to the ability of a given solvent to dissolve the intended polymer. A poor quality solvent will separate individual molecules, but each molecule will coil. A good solvent will separate each molecule such that the molecules approach their full, extended lengths. The degree of separation between molecules is not only impacted by solvent quality, but also by the solution concentration. High concentration will result in a high degree of polymer chain entanglement, while low concentration will result in low polymer chain entanglement. Temperature will affect solvent quality and polymer viscosity, and therefore temperature will also affect entanglement; though, electrospinning is often done at room temperature to remove this variable from the process. These solution parameters all determine the ability of the polymer solution to form and maintain a solid jet once ejected from the syringe. According to Shenoy, et. al, approximately 1-2 entanglements are required per chain for stable jet and fiber formation (Shenoy, Bates and Frisch). In the case of poly(L-lactic acid), Tan et. al found that the polymer's molecular weight, solution concentration, and solution conductivity were the dominant parameters that determined fiber morphology (S-H. Tan).

Process parameters are those specific to the electrospinning method and equipment (Salem). When a polymer solution droplet is formed at the tip of the electrospinning needle, it encounters the applied voltage. The charged solution droplet begins to elongate towards a grounded substrate as a means of discharging. This elongated droplet is referred to as a Taylor Cone. The droplet continues to elongate towards the grounded substrate until it forms a fiber jet. The jet undergoes bending instability because of charge imbalances on its surface, which cause the jet to travel in a random whipping motion. The whipping motion is quite critical to the fiber formation process because it extends the path between the needle and the collector so that the solvent can evaporate to form a solid fiber, and it draws the fiber, narrowing the diameter and aligning molecules along the axis for improved strength. Flow rate through the needle determines the size of the droplet formed. Applied voltage determines Taylor Cone quality and jet whipping. Needle to collector distance affects the applied voltage across the jet. In order to form a Taylor Cone and eventually a fiber, these three parameters must be balanced. A high flow rate will result in a solution droplet that is too heavy to be elongated by the applied voltage. Too low of a flow rate will result in sparking between the needle and collector or electrospray. Too high applied voltage will result in electrospray or sparking as well. Too little applied voltage will fail to form a Taylor Cone and jet all together. Too small needle to collector distance will result in sparking, while too large of a distance will prevent the solution from discharging via fiber formation. Jet instability produces beaded fibers (Weiwei Zuo).

Modifying the Fibers

It is possible to modify electrospun fibers by altering spinning equipment, conditions or content. Examples of alternative spinning equipment include temperature controlled setups, magnetic coils and modified substrates.

Heated and cooled electrospinning setups change final fiber properties by changing the spinning solution viscosity so that the solution behaves differently during the process. In the case of heating, the viscosity is decreased to produce a narrower jet, and thus, finer diameter fibers. Cooled setups increase solution viscosity to improve jet solidity during spinning. Temperature controlled setups can also be utilized to balance solution gelation for improved spinnability (Shenoy, Bates and Wnek, Correlations Between Electrospinnability and Physical Gelation). Gel-forming solutions can become too viscous to spin; however, careful balance of spinning parameters can produce acceptable fibers (Yanzhong Zhang).

Magnetic coils modify the electric field around a forming fiber such that the fiber travels in a predictable rather than random path towards the substrate. Although predictability may be useful to researchers or fiber producers, a controlled, essentially straight line path does not draw the fibers to improve mechanical properties via whipping motion.

Although the whipping path and thus fiber deposition occurs randomly given regular substrate and a controlled, Fiber deposition occurs selectively, meaning that the majority of fibers produced in an electrospinning run will land on the oppositely charged or grounded substrate because this is the most energetically favorable location. The spaces between deposited fibers are referred to as inter-fiber pores. Because of the random nature of the whipping and deposition processes, a range of inter-fiber pore sizes are observed. Typically, these pore sizes are measured and reported as average values. The pore sizes produced depend on the mass of polymer

deposited, the area over which it is deposited, and the polymer fiber dimensions. As reported previously by this research group, holding mass constant while thinning and elongating the fibers results in smaller inter-fiber pores and vice versa (D. Li).

Fiber Fillers: Conductive and Ionic Fillers

Ionic materials can be added to a polymer solution to improve the solution's conductivity. Conductivity contributes to spinnability, which usually results in fiber diameter reduction. Qin, et. al found that a variety of salt additives improve spinnability and reduce fiber diameter by varying degrees in electrospun Polyacrylonitrile solutions (Xiao-Hong Qin). In the case of poly(lactic-co-glycolic acid), researchers found that small amounts of the ionic additive benzyl triethylammonium chloride produced reduced fiber diameter and improved fiber morphology (Young You). As a result of improved solution conductivity, a lower polymer concentration may be used, which will result in a still finer fiber diameter because lower concentration solutions are less viscous (Matthew G. McKee).

Porous Fibers

Megelski et. al theorized that intra-fiber pore formation results from rapid solvent evaporation along with water droplet formation on the fibers during the spinning in atmospheric conditions (Silke Megelski).

Hollow Fibers

One of the most common strategies for forming hollow electrospun fibers is coaxial electrospinning followed by removal of the core. In coaxial electrospinning, two polymer solutions are fed into a single needle before being electrospun. The resulting fiber has a layered core-sheath structure. It is possible to control the thickness of these layers by adjusting the feed rate of the inner

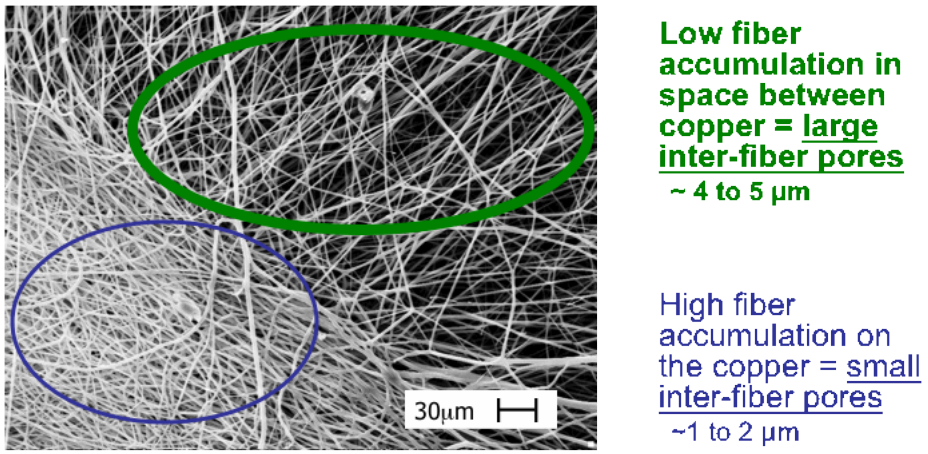

Figure 1 Selective deposition on copper grid and the resulting differences between inter-fiber pore sizes

solution component (Hongliang Jiang). Core diameter and whole fiber diameter can also be modified by varying inner solution concentration (Bin Sun). For successful separation between the layers, it is necessary to choose immiscible solutions with low interfacial tension (Bin Sun).

Hypotheses:

Selective Deposition

The concept of selective deposition is a critical one to this project. These authors propose that the use of a grid style collection substrate will result in high fiber deposition on the conductive grid components with low fiber deposition between the conductive grid components (Image 1). When compared with a flat control collection substrate, capillary flow porometry testing will verify this selective grid deposition by showing that large grids produce relatively large pores, a wide range of pore sizes, and a distinct bimodal pore size distribution. Small grids will produce relatively small pores, a narrow range of pore sizes, and a less distinct pore size distribution. Medium grids will produce pore sizes, pore size distributions and bimodal character between those produced by large and small grids. Selectively deposited fibers could be useful in tissue growth

applications needing spatially controlled patterns (Margaret W. Frey). Fiber length can be used to further control inter-fiber pore sizes such that high fiber length produces smaller pores and vice versa (M. W. Dapeng Li).

Electrospun fiber membranes collected on gridded substrates will be further compared with wettability testing. Wettability is the process in which liquid travels up a hanging strip of material over a given period of time. The amount of liquid absorbed by the fabric is quantified with incremental weight measurements over time. Wettability relies heavily upon capillary action. In an electrospun fabric, inter-fiber pores serve as capillaries. It is hypothesized that a large number of small pores, as expected in small grid samples, will result in more rapid liquid uptake because of the abundance of viable flow paths, and vice versa.

Motivation

This electrospun membrane could be utilized in tissue engineering applications. Topographical features of tissue engineering scaffold determine cell spreading, orientation and proliferation (Anand S. Badami). Endothelial vascular cells demonstrate substrate roughness sensitivity, growing better on smooth surfaces than on rough surfaces (Chengyu Xu). However, cells can grow better on electrospun fibers than on smooth surfaces if the fibers are of an appropriate diameter such as 2.1 μm as demonstrated by Badami, et. Al (Anand S. Badami). In the case of blood vessel tissue engineering, it is desirable to have areas of aligned fibrous scaffold to mimic natural extracellular matrix architecture (C.Y. Xu). Specifically, appropriate spatial organization on the mesoscopic scale is a critical design component of artificial extracellular matrices for tissue engineering (Satoru Kidoaki). The ideal tissue growth scaffold should have appropriate microarchitectures, well-controlled pore sizes and porosity, and biocompatibility to produce the desired cell growth along with nutrient supply and vascularization of cells (Dasai). Biocompatible PLA electrospun

selectively onto an appropriately patterned surface under controlled conditions has the capability of meeting these scaffold requirements.

Compliance

Compliance is the mathematical inverse of modulus, a mechanical property determined with tensile testing. Put simply, compliance is the ability of a material to adjust to load. These authors hypothesize that reductions in fiber mass such as those in porous fibers, hollow fibers and fine fibers result in improved compliance. Sun, et. al demonstrated that core-shell electrospun poly(vinyl pyrrolidone) and PLA have reduced tensile strength and modulus as compared to PLA alone (Bin Sun).

Motivation

In addition to improving compliance for possible improved cell adhesion in tissue growth applications, reduced fiber volume increases surface area for biosensing applications while utilizing less material (Dapeng Li). Mechanical signals influence cell proliferation, so it follows that regulating fiber mechanical properties may be useful in tissue engineering application in which cell growth must be controlled (A.J. Putnam).

Materials

Commercial grade Polylactic acid (PLA) polymer (M_w = 186,000 and 211,000 Da, density = 1.25 g/cm^3) was supplied by Cargill Dow (Minnetonka, MN). Chloroform and acetone were purchased from VWR Scientific (West Chester, PA). Medical grade PLA (manufacturer product 100 DL 7E) was purchased from Lakeshore Biomaterials, Inc. (Birmingham, AL). *N*,*N*-Dimethyl formamide (DMF) was purchased from Fisher Scientific (Pittsburg, PA). Galwick oil (15.9 Dynes/cm) was purchased from Porous Materials, Inc. (Ithaca, NY). Hexane was purchased from Fisher Scientific (Pittsburg, PA). All reagents are used without further purification.

Experimental

Medical grade PLA was dissolved in DMF. Commercial grade PLA was dissolved in chloroform and acetone. The resulting PLA solutions were and electrospun at a rate of 0.01 ml/min for 20 minutes with a 20 gauge needle at 10-20kV and 10cm distance between needle and collector. Collectors included flat copper plate, and small, medium and large grids in which copper wire was arranged with 1, 3 and 5 mm spacing between the wires. After collection, the membranes were allowed to dry at least overnight before being separated from the substrate for testing.

Porometry was performed with a PMI, Inc. Capillary Flow Porometer. Samples were cut into 3cm by 3cm squares, placed in the porometer test chamber disc, secured with an o-ring, wetted with Galwick oil, and tested using the Wetup/Dryup test method provided in the accompanying software package.

Wettability was performed using a wetting balance. Samples were cut into 3cm by 0.5cm rectangles, glued with fabric glue to wire hooks, and allowed to cure 24 hours before testing. To test, a sample was suspended above a dish of hexane, lowered towards the surface of the liquid until contact was made, and the sample was weighed every 0.6 seconds for 20 minutes to determine the mass hexane absorbed over time.

Instron tensile testing was performed according to ASTM D638-02a. A metal dogbone cutter shape was produced at the machine shop according to the dimensions required by ASTM D638-02a (3.18mm wide, 3.53mm long). Samples were cut using the resulting dogbone cutter and a hand press. A tensile strain rate of 1mm/min was applied.

Results and Discussion

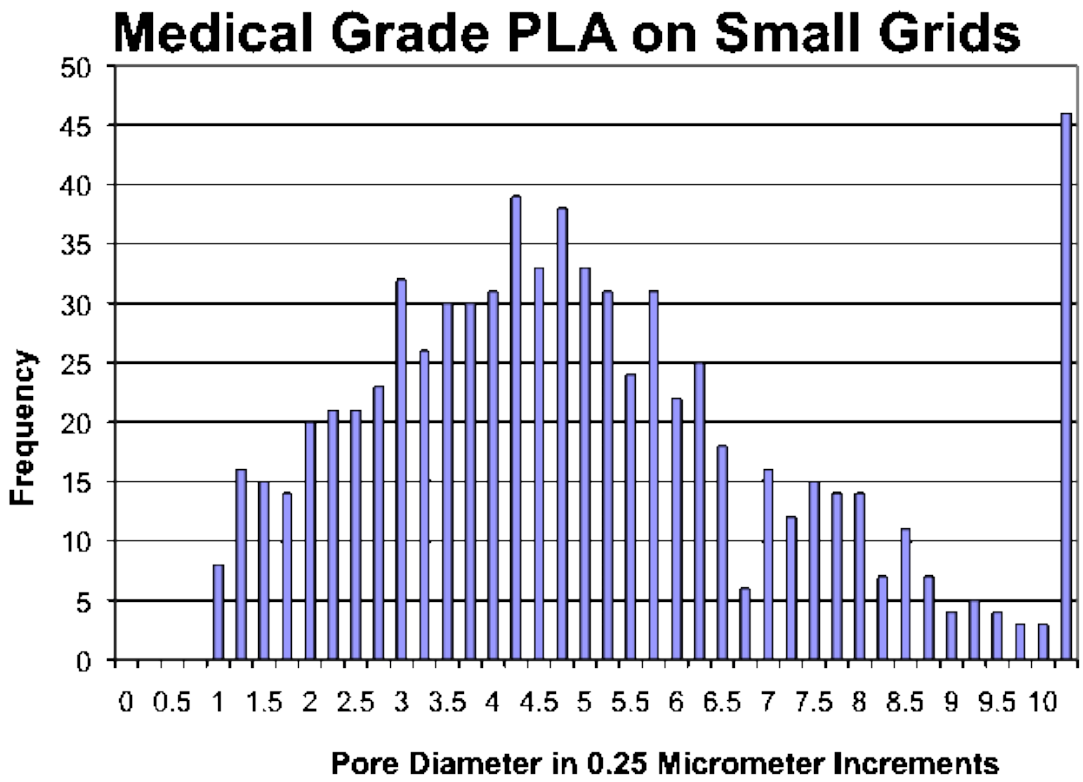

Figure 2 Medical Grade PLA on Small Grids: Frequency vs. Pore Diameter in 0.25 Micrometer Increments

Electrospinning on a small grid substrate produced a pore structure similar to flat substrate spinning. This approximately unimodal pore size distribution occurred because the tight wire structure caused the fibers to deposit fairly evenly across the surface.

Figure 3 shows the number of average pore sizes recorded in 0.25 micrometer increments. Each sample displays two distinct modes, showing that a bimodal pore size distribution is achieved. Arranged in order of increasing weight, it is also confirmed that pore size decreases with increasing sample weight because more fibers result in smaller inter-fiber pores. The average difference between small and large pore size modes is 1.92 micrometers, and the ANOVA PValue 9.33E-22 verifies that these small and large modes are distinct.

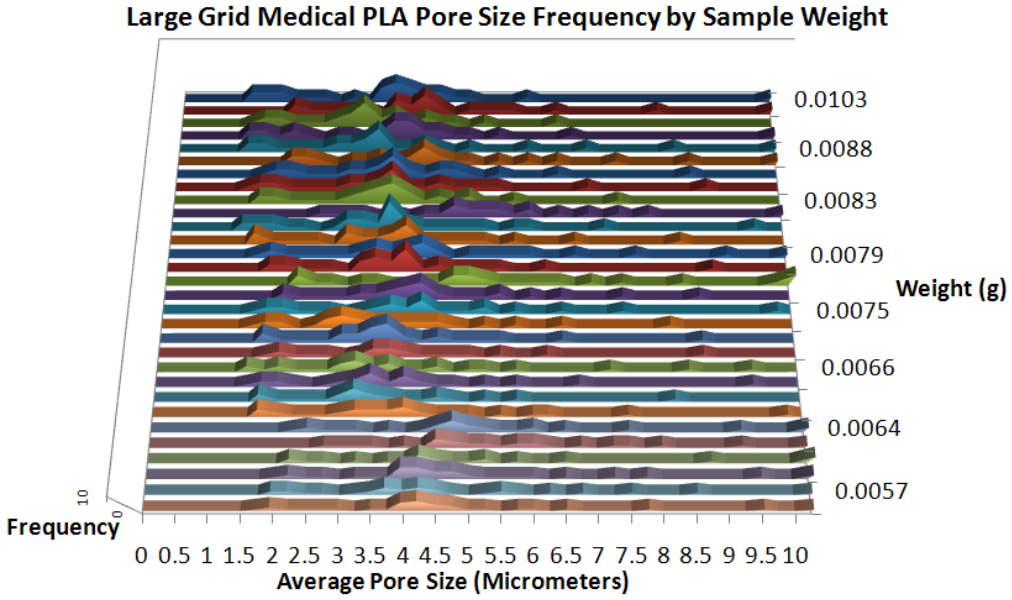

Figure 3 Frequency of Pore Sizes in Large Grid Medical PLA According to Sample Weight

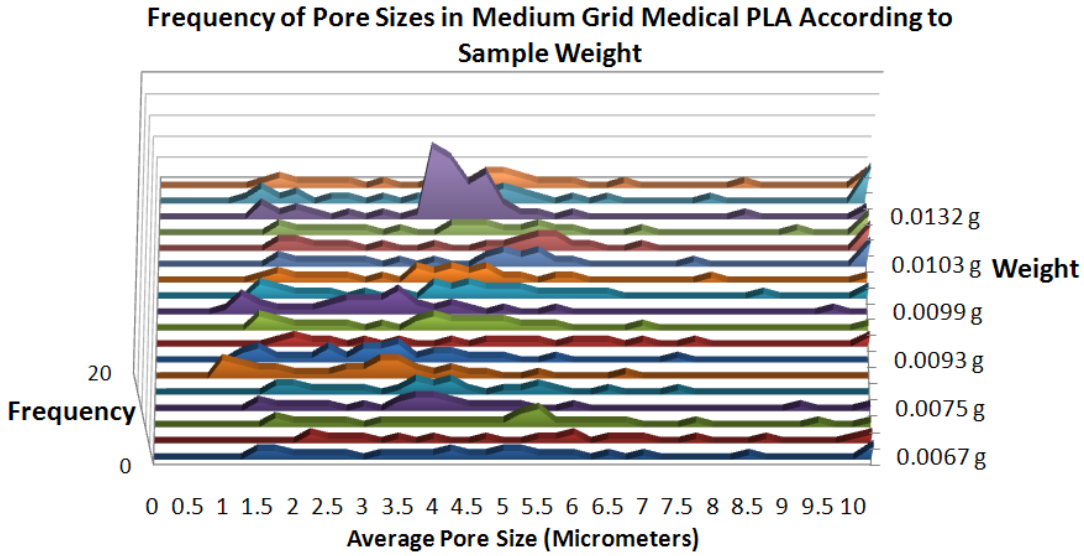

Figure 4 Frequency of Pore Sizes in Medium Grid Medical PLA According to Sample Weight

Figure 4 demonstrates the same bimodal pore size phenomenon illustrated in the large medical histogram. The distinction here is simply that the modes are farther apart, as expected with larger spaces between collection zones. ANOVA P-value 1.51E-16 verifies that small and large modes are distinct.

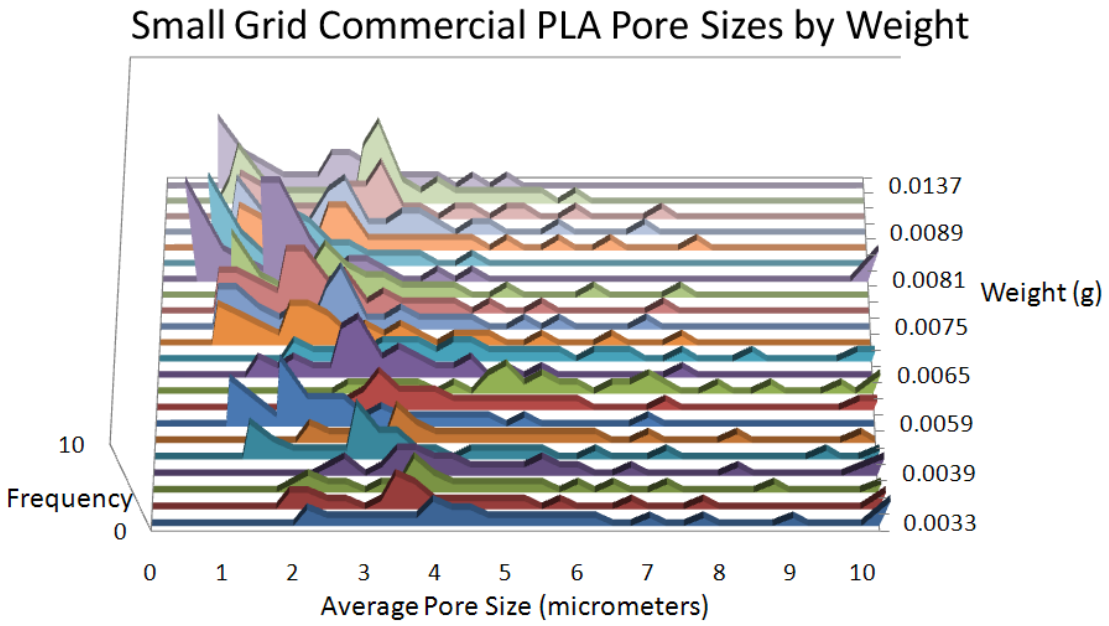

Figure 5 Commercial Grade PLA on Small Grid

Unlike medical grade PLA, electrospinning commercial grade PLA on a small grid does produce a bimodal pore size distribution with two distinct modes as verified by ANOVA P-value 2.1E-9. It is likely the difference in polymer chain length that causes this. Medical PLA's number average molecular weight is near 10,000, which is the minimum required for fiber formation via appropriate chain entanglements. Commercial PLA's number average molecular weight is approximately 80,000, which produces a more consistent fiber with less breakage because the chains are long enough to entangle appropriately.

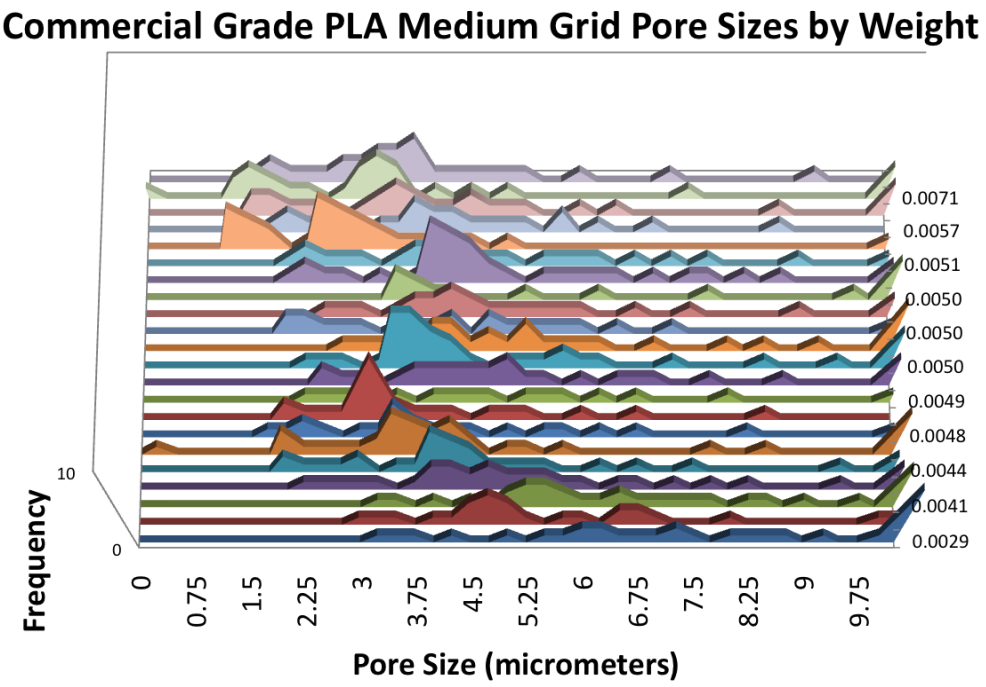

Figure 6 Commercial Grade PLA on Medium Grid by Weight

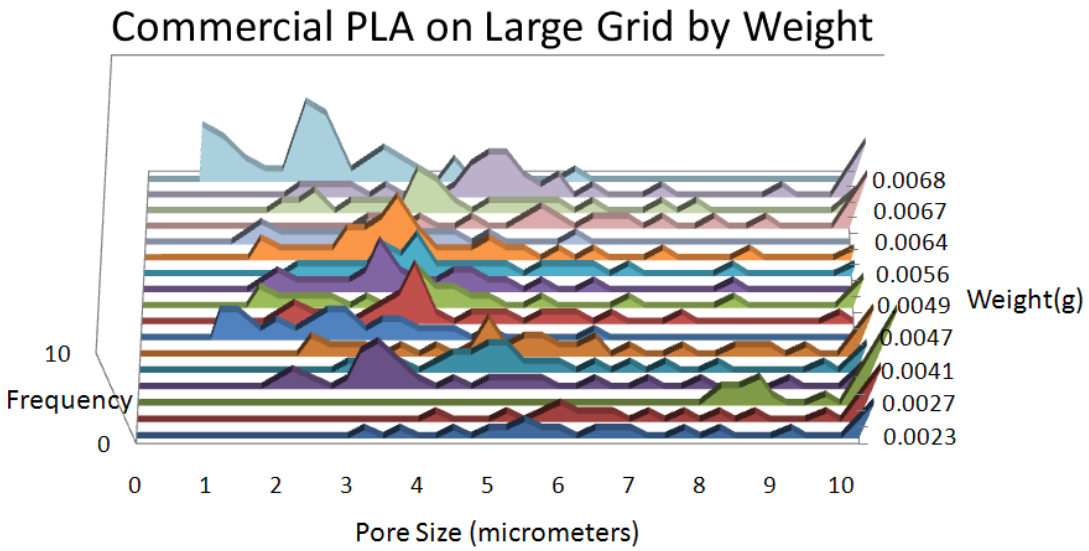

Figure 7 Commercial PLA on Large Grid by Weight. Large grid electrospun PLA also produces a bimodal pore size distribution. Results vary from sample to sample; however, ANOVA P-value 0.005 between the modes verifies that the modes are distinct.

Electrospinning commercial PLA on a medium grid results in a bimodal inter-fiber pore size distribution. It appears as though the small and large modes are more distinct than those form with medical PLA on medium grid ANOVA P-value 3.97E-9 between the modes verifies that the modes are unique from one another.

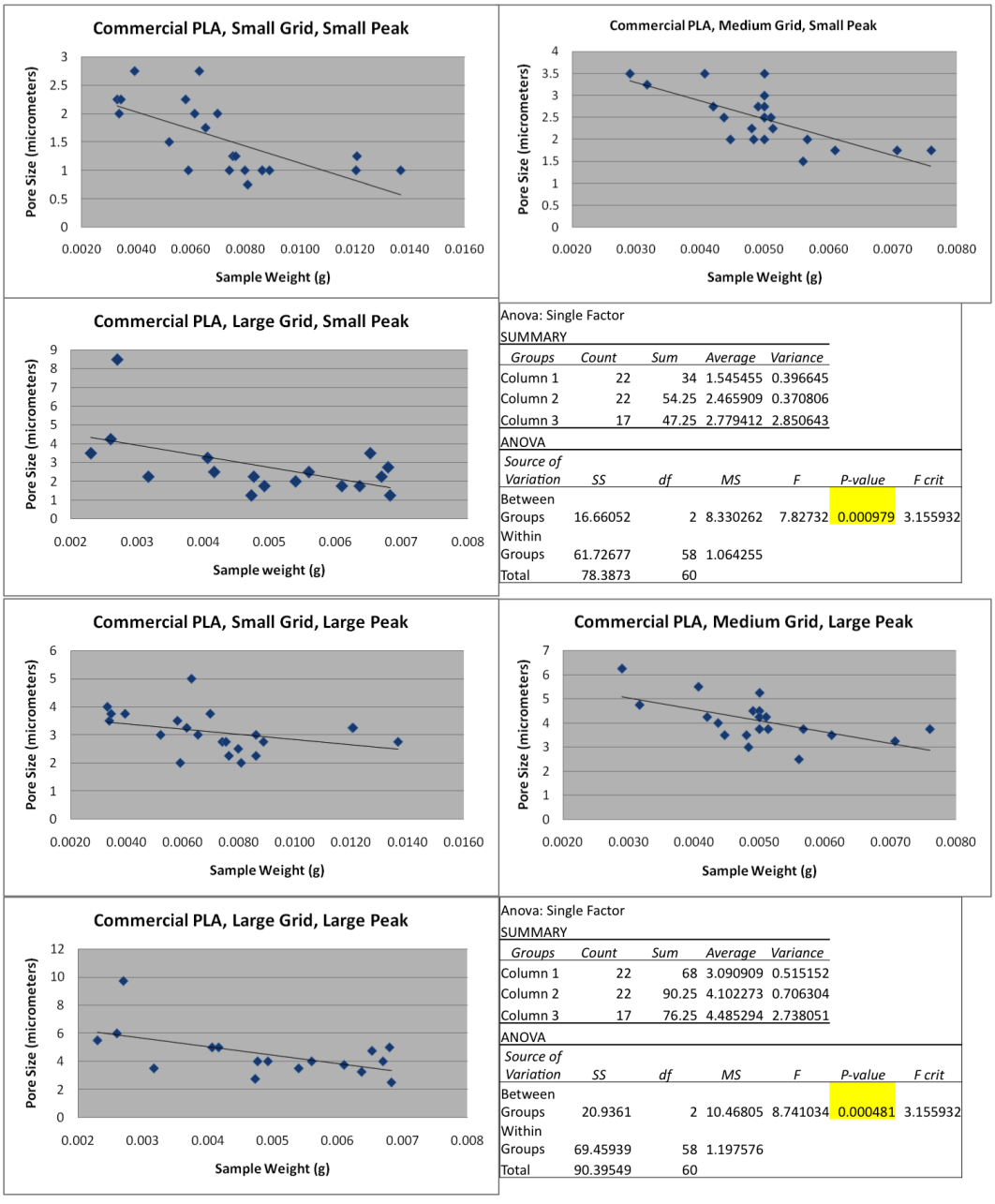

Figure 8 Small & Large Peak Comparison Between Grid Sizes, Commercial PLA

Comparing small peaks between grid sizes shows that the small pore size does depend on the overall grid stucture onto which fibers are deposited. ANOVA P-value 0.0009 between each of the small mode data sets shows that the small pores are distinct. This phenomena is also observed with the large modes, and the corresponding ANOVA P-value is 0.0005. The confidence level for these analyses is 95%.

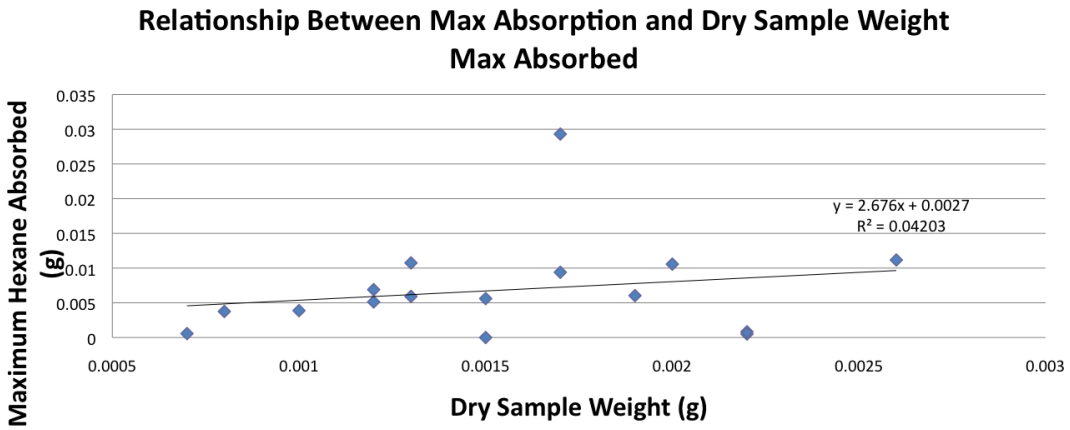

Figure 9 Medical PLA Wettability Medium Grid

The plot of hexane absorbed vs. dry sample weight shows that the amount of liquid absorbed by the sample corresponds to dry sample weight. This is logical because the greater the sample weight, the more fibers present, and the smaller the inter-fiber pores. In this scenario, small inter-fiber pores act as capillaries that draw liquid into the fiber membrane. There is no observed relationship between liquid absorbed and the largest pore size on a given membrane, though. This observation is logical because it is all of the inter-fiber pores together that determine how much liquid will be observed, and because small pores have a greater impact on absorbency than large pores because of the greater capillary action produced by small pores.

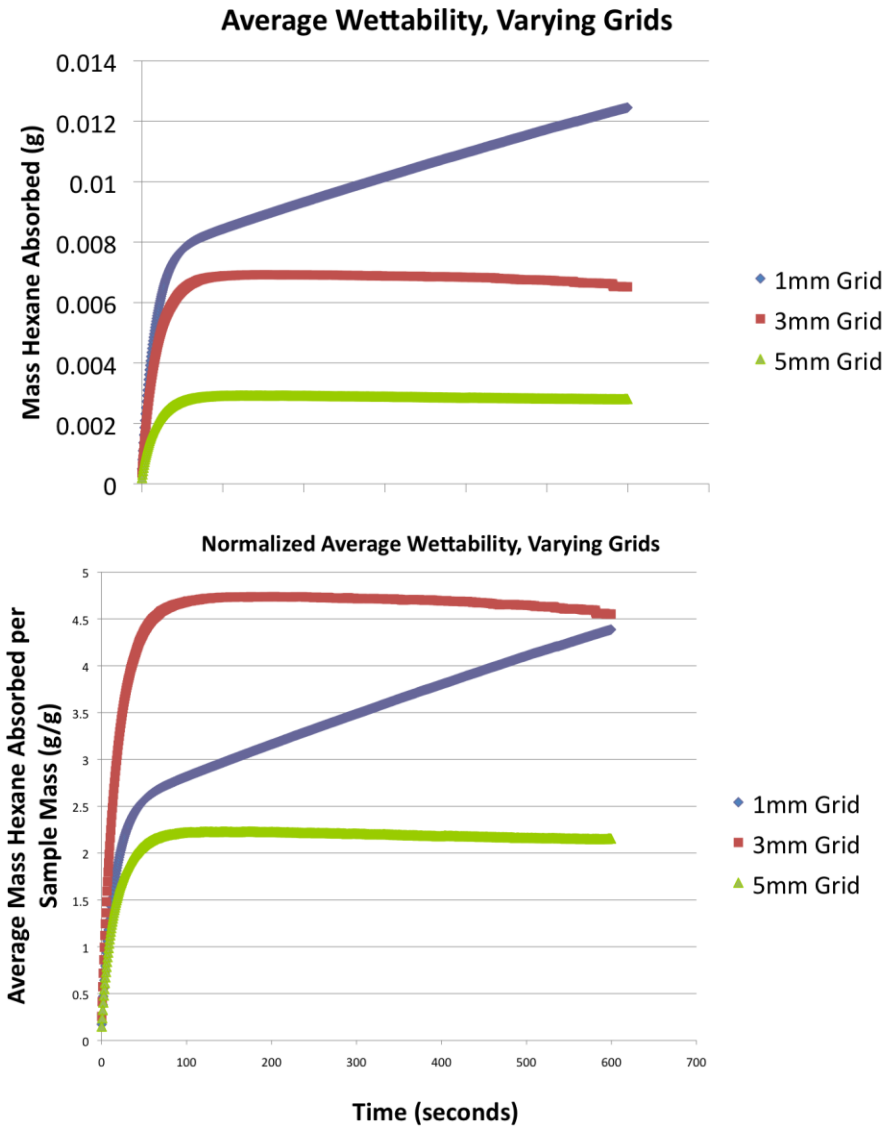

Figure 10 Medical PLA Wettability: Varying Grid Sizes

Medical PLA small grid wettability shows steadily increasing liquid absorption. These results are consistent with wettability curves for typical electrospun membranes with unimodal inter-fiber pore size distributions. In the case of grid spun membranes with bimodal pore size distributions, namely medium and large grid membranes, a wide pore size distribution results in both increasing and decreasing absorption. This reduction in weight absorbed is likely a result of evaporation from the larger pore

sections that have relatively less capillary action and therefore less ability to prevent the hexane from evaporating at extended lengths of time. In the case of the medium grid, a nearly vertical jump in absorbency was observed with every trial. This jump likely occurred because the medium grid demonstrated the most distinct small and large pores, which would have different absorbency characteristics. The jump occurs at a distinct point in time because the liquid first travels easily through the smaller capillaries, then fills in the larger capillaries.

Comparing the small, medium and large grid membranes to each other shows that small and medium grids absorb approximately the same maximum amount of liquid per unit weight of dry sample. Medium grids absorb relatively quickly, while large grids absorb less liquid overall. ANOVA P-value between the max absorbed for each of the membranes shows that they have distinct maximum absorption capabilities, with large absorbing 4 times its weight, small absorbing 6 times its weight, and medium absorbing 8 times its weight in hexane.

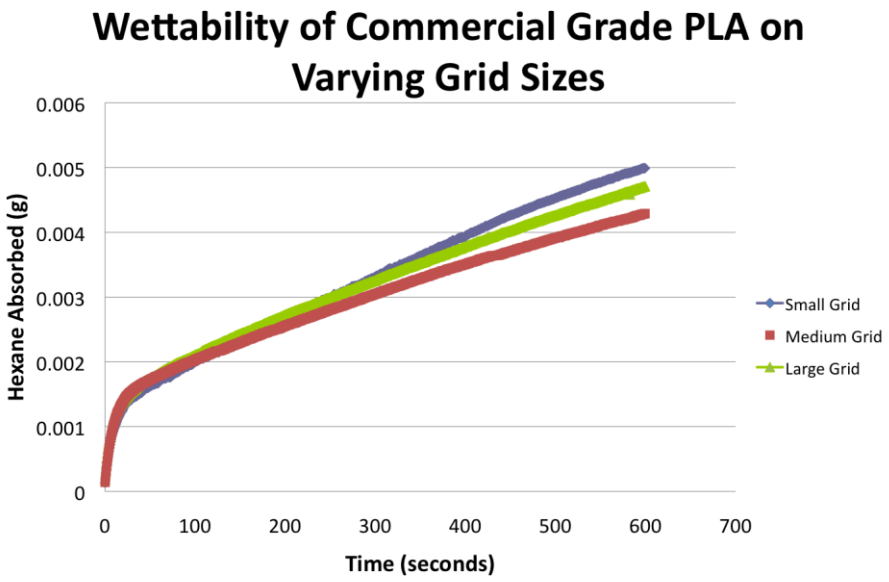

Figure 11 Commercial PLA Wettability: Varying Grid Sizes

The wettability capabilities of small, medium and large grid membranes spun from commercial grade PLA are roughly the same. ANOVA between the maximum hexane absorbed does not show distinct absorption capabilities between the samples.

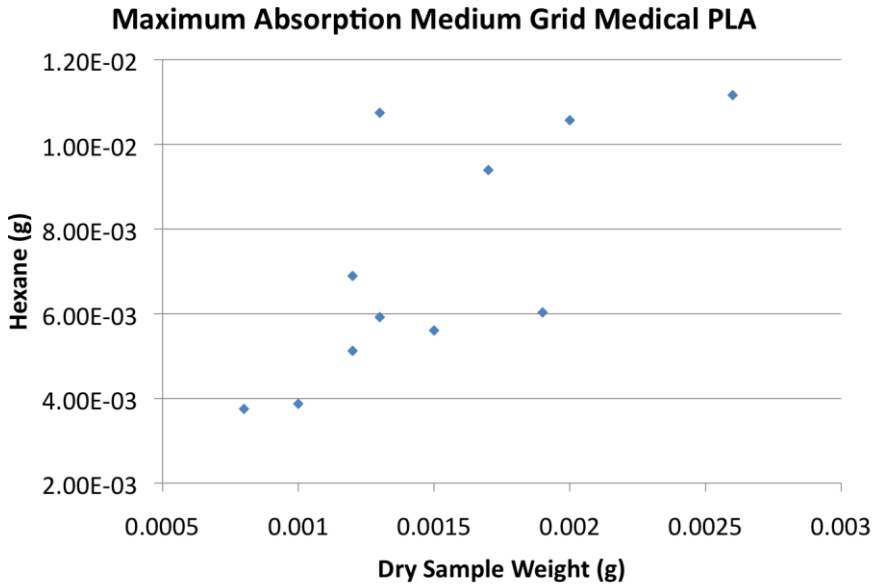

Figure 12 Comparing Max Absorption of Medical and Commercial PLA

Small and large membranes of medical and commercial PLA demonstrate distinctly different maximum absorption capabilities. Medium membranes of commercial and medical PLA absorb approximately the same maximum amount of liquid during wettability testing with hexane.

The capillary flow equation is based on the surface tension of the wetting liquid, the contact angle the liquid makes with the pore, and the physical size of the pore. The equation can be rearranged to solve for the mass of liquid absorbed by a single pore of a given size. The pores can be modeled as a series of interconnected spheres because approximately random fiber deposition leads to irregularly shaped volumes between fibers. The final equation is the sum of hexane absorbed by all pores of each size.

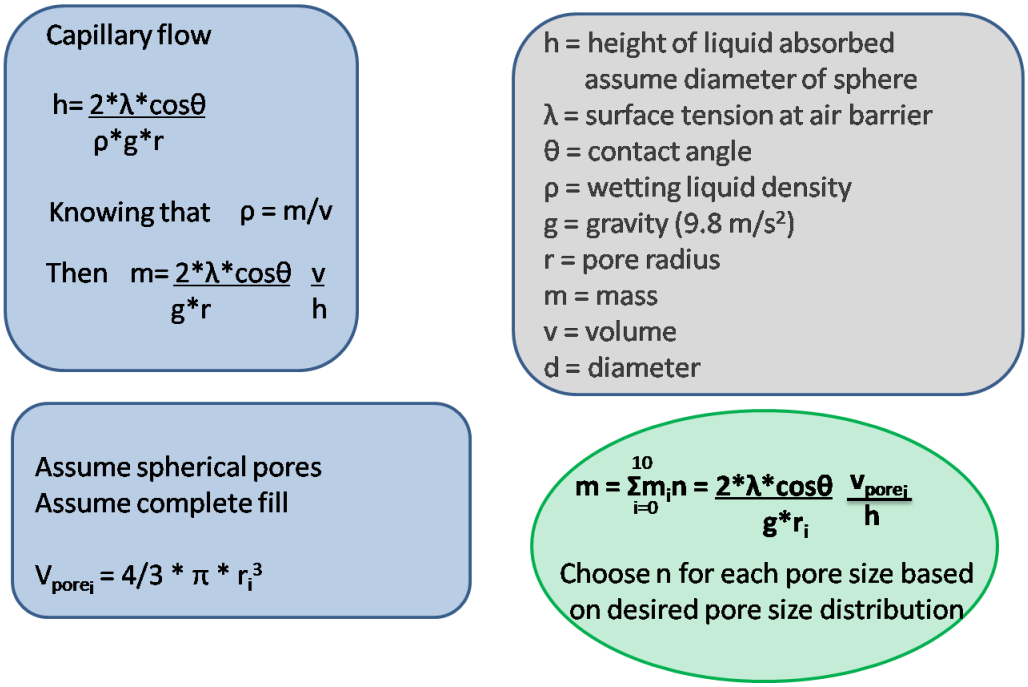

Figure 13 Mathematical prediction of absorbency from pore size distribution

The only remaining challenge is approximating the pore number. In both the rectangle-based approximation and the ImageJ-based approximation described below, pore number is most greatly influenced by sample thickness, while grid size becomes nearly negligible. In general, electrospun membrane thickness is difficult to approximate because of the randomness of fiber deposition and variation in fiber thickness. In the case of grid electrospinning, thickness is even more variable because most fibers deposit on the copper wire sections, resulting in a membrane that has sections with only one or two layers of fibers in thickness adjacent to sections with many layers of fibers in thickness.

The number of pores critical to wetting behavior is not closely predicted using sample shape and porometry results. This author attempted to approximate each pore number by calculating the total pore volume based on sample and fiber dimensions, then using porometry data to determine the fraction of total pore volume taken up by

each pore diameter. The resulting pore number calculation differed from the measured effective number by orders of magnitude, and was not significantly different between small, medium and large grids.

Alternatively, this author attempted to approximate pore number using SEM images and ImageJ software to determine the area of the pores in a 2-dimensional image, then multiplying the resulting area by the approximate thickness of the sample to determine the total pore volume. The resulting total pore volume was multiplied by the fraction of each pore diameter as determined by pore size distributions from porometry. The results of the ImageJ-produced pore number approximation were also off by orders of magnitude, and not significantly different between small, medium and large grids.

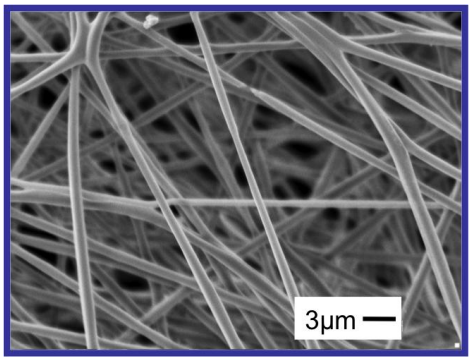

CONTROL

•Medical Grade PLA:DMF 9:16 w/w

•0% NaCl w/w

•Average fiber diameter =0.976µm from n=50 measurements

ANOVA **Comparing 9:16 to 9:16 with 20%NaCl**

Source of Variation	*SS*	*df*	*MS*	*F*	*P-value*	*F crit*
Between Groups	8.099716	1	8.099716	207.0573	6.65E-26	3.938111
Within Groups	3.833587	98	0.039118			
Total	11.9333	99				

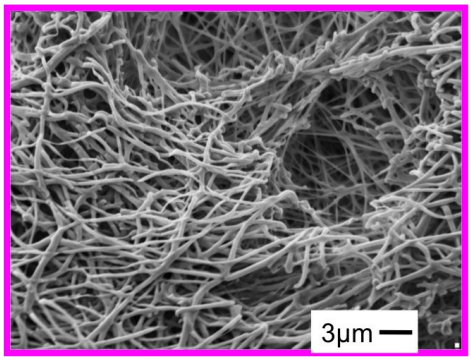

9:16 PLA:DMF with 20%NaCl

•Medical Grade PLA:DMF 9:16 w/w

•20% NaCl w/w

•Average fiber diameter =0.407µm from n=50 measurements

57.9% Reduction in fiber diameter compared to control 9:16 PLA:DMF

Figure 14 Comparing Control Medical PLA Fibers with Medical PLA Fibers Plus Sodium Chloride

The control sample demonstrates consistent fiber morphology. The addition of sodium chloride to the spinning solution reduced the fiber diameter compared to the control, but produced inconsistent fiber morphology.

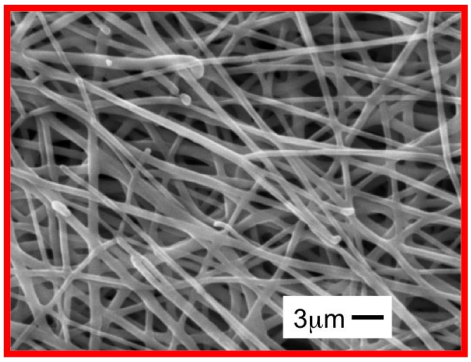

9:16.8 PLA:DMF with no salt

•Medical Grade PLA & 5% increase in solvent DMF compared to control

•0% NaCl w/w

•Average fiber diameter =0.710µm from n=50 measurements

26.6% Reduction in fiber diameter compared to control (9:16 PLA:DMF)

ANOVA Comparing 9:16.8 with no salt to 9:16.8 with 23%NaCl						
Source of Variation	*SS*	*df*	*MS*	*F*	*P-value*	*F crit*
Between Groups	5.962098	1	5.962098	274.6212	6.51E-30	3.940163
Within Groups	2.084185	96	0.02171			
Total	8.046283	97				

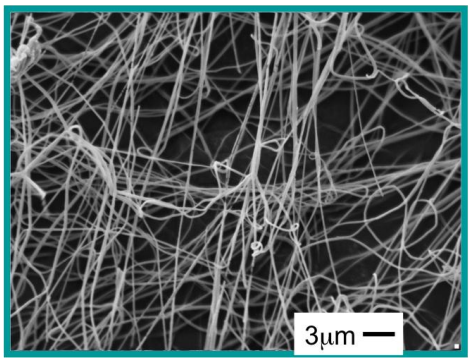

9:16.8 PLA:DMF with 23%NaCl

•Medical Grade PLA & 5% increase in solvent DMF compared to control 9:16.8 PLA:DMF with 23% NaCl

•Average fiber diameter =0.214µm from n=50 measurements

69.9% Reduction in fiber diameter compared to 9:16.8 PLA:DMF

77.7% Reduction in fiber diameter compared to control 9:16 PLA:DMF

Figure 15 Comparing Medical PLA Fibers Plus Additional Solvent to Medical PLA Fibers Plus Additional Solvent and Sodium Chloride

Additional solvent alone compared to the control produced reduced fiber diameter, but produced inconsistent fiber morphology. Additional solvent plus the addition of sodium chloride to the spinning dope produced reduced fiber diameter as compared to the control and as compared to increased solvent alone; however, the resulting fibers had inconsistent morphology.

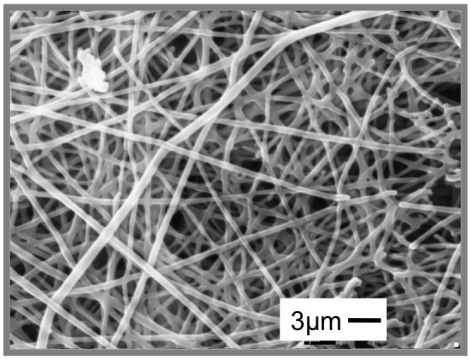

9:17.2 PLA:DMF with no salt

•Medical Grade PLA & 7.5% increase in solvent DMF compared to control

•0% NaCl w/w

•Average fiber diameter =0.484µm from n=50 measurements

49.9% Reduction in fiber diameter compared to control 9:16 PLA:DMF

ANOVA Comparing 9:17.2 with no salt to 9:17.2 PLA:DMF with 25%NaCl

Source of Variation	SS	df	MS	F	P-value	F crit
Between Groups	0.94634	1	0.94634	60.96632	6.5E-12	3.938111
Within Groups	1.521189	98	0.015522			
Total	2.467529	99				

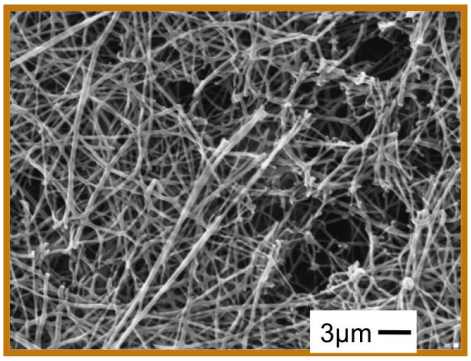

9:17.2 PLA:DMF with 25%NaCl

•Medical Grade PLA & 7.5% increase in solvent DMF compared to control

•25% NaCl w/w

•Average fiber diameter =0.289µm from n=50 measurements

40.3% Reduction in fiber diameter compared to 9:17.2 PLA:DMF no salt

70.1% Reduction in fiber diameter compared to Control 9:16 PLA:DMF

Figure 16 Comparing Maximum Solvent Fibers with Maximum Solvent Plus Sodium Chloride Fibers

Fibers produced from spinning dopes containing maximum solvent and maximum solvent plus sodium chloride both demonstrated reduced fiber diameter compared to the control, but they also demonstrated inconsistent morphologies.

It is seen in Figure 17 scanning electron microscopy images that although fibers electrospun at varying applied voltages had similar fiber diameters, they did demonstrate varying morphology as a result of applied voltage. Fibers electrospun at 10kV demonstrate a dimpled surface. Fibers electrospun at 15kV demonstrate a smooth surface and approximately circular cross section. Fibers electrospun at 20kV demonstrate a slightly scaled surface and irregular cross section.

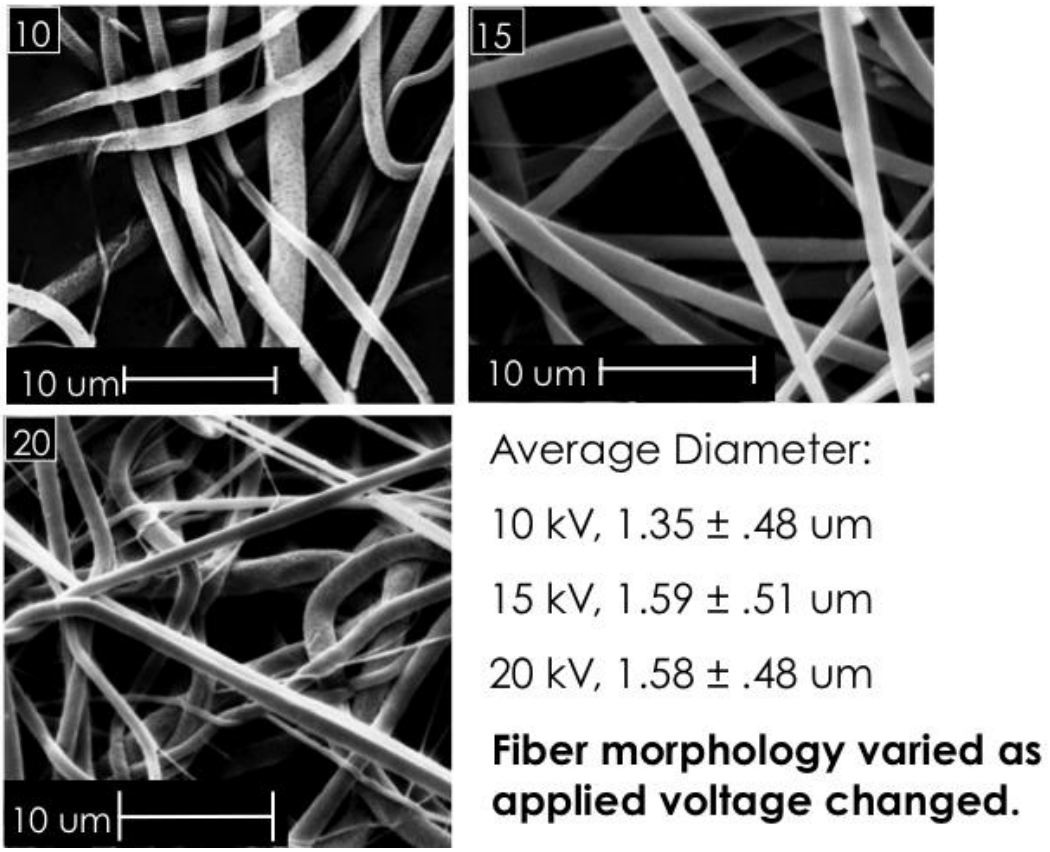

Figure 17 Comparing Fiber Morphology in Commercial PLA

Table 1 Comparing Compliance in Commercial PLA

ANOVA: Commercial Grade PLA Compliance by Voltage	
Voltages Compared	P-value in 95% Confidence Interval
10kV, 15kV	**0.701958268**
15kV, 20kV	**0.178012568**
10kV, 20kV	**0.173243907**

ANOVA was used to compare the compliance of commercial grade PLA electrospun at 10kV, 15kV and 20kV. Within a 95% confidence interval, it is shown that varying applied electrospinning voltage does not significantly affect compliance.

Statistical Significance of the Data

In order for the data to be considered statistically significant, a normal distribution must be analyzed. Specifically, a minimum of 30 samples is necessary. Although 30 samples were not studied for each test, the results are consistent, and can therefore be used as indicators of statistically significant results if the minimum sample number were used.

Conclusions

Electrospinning onto a patterned surface is a valid technique for producing membranes with varying pore size/distribution. The porometry data and ANOVA analysis shows that electrospinning onto a grid creates a bimodal pore size distribution. Furthermore, large grids have the largest modes and a large gap between modes, medium grids have mid level modes and mid level gap between modes, and small grids have the smallest modes and narrowest gap between modes.

Inter-sample pore size variation impacts membrane wettability. It is demonstrated that small pore sizes combined with a narrow gap between pore size modes result in more rapid liquid uptake, and vice versa.

Absorbency can be predicted by modeling the pores as a series of interconnected spheres. Modifying the capillary flow equation for spherical pores and iterating the equation over the range and frequency of pore sizes in a given membrane produces a reasonably accurate absorbency prediction.

Variations in fiber qualities were achieved by altering applied electrospinning voltage, ionic filler content and solvent concentration. None of the variations in fiber morphology or ionicity impacted the mechanical membrane property compliance. This consistency in compliance likely resulted because load sharing during tensile testing was not significantly altered by slight fiber variations.

WORKS CITED

Bin Sun, Bin Duan, Xiaoyan Yuan. "Preparation of Core/Shell PVP/PLA Ultrafine Fibers by Coaxial Electrospinning." Journal of Applied Polymer Science 102 (2006): 39-45.

D. Li, Y.L. Joo, M.W. Frey. "Characterization of Nanofibrous Membranes by Capillary Flow Porometry." Journal of Membrane Science 286 (2006): 104-114.

Dapeng Li, Margaret W. Frey, Antje Baeumner. "Electrospun Polylactic Acid Nanofiber Membranes as Substrates for Biosensor Assemblies." Journal of Membrane Science 279 (2006): 354-363.

Gladding, Ernest K. Patent 2168027. 1939.

Hongliang Jiang, Yingqian Hu, Yan Li, Pengcheng Zhao, Kangjie Zhu, Weiliam Chen. "A Facile Technique to Prepare Biodegradable Coaxial Electrospun Nanofibers for Controlled Release of Bioactive Agents." Journal of Controlled Release 108 (2005): 237-243.

Margaret W. Frey, Dapeng Li, Tina Tsong, Antje J. Baeumner, Yong L. Joo. "Incorporation of Biotin into PLA Nanofibers via Suspension and Dissolution in the Electrospinning Dope." Journal of Biobased Materials and Bioenergy 1 (2007): 219-227.

Matthew G. McKee, Matthew T. Hunley, John M. Layman, Timothy E. Long. "Solution Rheological Behavior and Electrospinning fo Cationic Polyelectrolytes." Macromolecules 39 (2006): 575-583.

Salem, David R. Structure Formation in Polymeric Fibers. Munich: Hanser, 2001.

S-H. Tan, R. Inai, M. Kotaki, S. Ramakrishna. "Systematic Parameter Study for Ultra-fine Fiber Fabrication via Electrospinning Process." Polymer 46 (2005): 6128-6134.

Shenoy, Suresh L., et al. "Role of Chain Entangelements on Fiber Formation During Electrospinning of Polymer Solutions: Good Solvent, Non-specific Polymer-Polymer Interaction Limit." Polymer 46 (2005): 3372-3384.

Shenoy, Suresh L., W. Douglas Bates and Gary Wnek. "Correlations Between Electrospinnability and Physical Gelation." Polymer 46 (2005): 8990-9004.

Silke Megelski, Jean S. Stephens, D. Bruce Chase, John F. Rabolt. "Micro- and Nanostructured Surface Morphology on Electrospun Polymer Fibers." Macromolecules 35 (2002): 8456-8466.

Weiwei Zuo, Meifang Zhu, Wen Yang, Hao Yu, Yanmo Chen, Yu Zhang. "Experimental Study on Relationship Between Jet Instability and Formation of Beaded Fibers During Electrospinning." Polymer Engineering and Science (2005): 704-709.

Xiao-Hong Qin, En-Long Yang, Ni Li, Shan-Yuan Wang. "Effect of Different Salts on Electrospinning of Polyacrylonitrile (PAN) Polymer Solutions." Journal of Applied Polymer Science 103 (2007): 3865-3870.

Yanzhong Zhang, Zheng-Ming Huang, Ziaojing Xu, Chwee Teck Lim, Seeram Ramakrishna. "Preparation of Core-Shell Structured PCL-r-Gelatin Bi-Component Nanofibers by Coaxial Electrospinning." Chemistry of Materials 16 (2004): 3406-3409.

Young You, Seung Jin Lee, Byung-Moo Min, Won Ho Park. "Effect of Solution Properties on Nanofibrous Structure of Electrospun Poly(lactic-co-glycolic acid)." Journal of Applied Polymer Science 99 (2006): 1214-1221.